AIAA 2001-3811

AN ANALYTICAL MODEL FOR THE IMPULSE OF A SINGLE-CYCLE PULSE DETONATION ENGINE

E. Wintenberger, J.M. Austin, M. Cooper, S. Jackson, and J.E. Shepherd
Graduate Aeronautical Laboratories, California Institute of Technology, Pasadena, CA 91125

37th AIAA/ASME/SAE/ASEE
Joint Propulsion Conference and Exhibit
July 8–11, 2001, Salt Lake City, UT

AN ANALYTICAL MODEL FOR THE IMPULSE OF A SINGLE-CYCLE PULSE DETONATION ENGINE

E. Wintenberger, J.M. Austin, M. Cooper, S. Jackson, and J.E. Shepherd
Graduate Aeronautical Laboratories, California Institute of Technology, Pasadena, CA 91125

An analytical model for the impulse of a single-cycle pulse detonation engine has been developed and validated against experimental data. The model analyzes the pressure differential at the thrust surface of the detonation tube. The pressure inside the tube is modeled with a constant pressure region and a blowdown process. A careful study of the gas dynamics inside the tube enables the derivation of a similarity solution for the constant pressure part. The blowdown process is modeled using dimensional analysis and empirical observations. The model predictions are validated against direct experimental measurements in terms of impulse per unit volume, specific impulse, and thrust. Impulse per unit volume and specific impulse calculations are carried out for a wide range of fuel-oxygen-nitrogen mixtures (including aviation fuels) varying initial pressure, equivalence ratio, and nitrogen dilution. The effect of the initial temperature is also investigated. Comparisons with numerical simulation estimates of the specific impulse are given.

Nomenclature

A	cross-sectional area of detonation tube
c_1	sound speed of reactants
c_2	sound speed of burned gases just behind detonation wave
c_3	sound speed of burned gases behind Taylor wave
d	inner diameter of detonation tube
f	cycle repetition frequency
g	gravity acceleration
I	single-cycle impulse
I_V	impulse per unit volume
I_{sp}	mixture-based specific impulse
I_{spf}	fuel-based specific impulse
K	proportionality coefficient
L	length of detonation tube
M_{CJ}	Chapman-Jouguet Mach number
P	pressure
P_0	pressure outside detonation tube
P_1	initial pressure of reactants
P_2	Chapman-Jouguet pressure peak
P_3	pressure of burned gases behind Taylor wave
t	time
t_1	time taken by the detonation wave to reach the open end of the tube
t_2	time taken by the first reflected characteristic to reach back the thrust surface
t_3	time associated with blowdown process
T	thrust
T_1	initial temperature of reactants
u	flow velocity
u_2	flow velocity just behind detonation wave
U_{CJ}	Chapman-Jouguet detonation velocity
V	inner volume of detonation tube
X_F	fuel mass fraction
α	non-dimensional parameter corresponding to time $(t_1 + t_2)$
β	non-dimensional parameter corresponding to blowdown process
ΔP	pressure differential
ΔP_3	pressure differential at the thrust surface
η	similarity variable
γ	ratio of specific heats
λ	cell size
ϕ	equivalence ratio
ρ_1	initial density of reactants

Introduction

A key issue[1–5] in evaluating pulse detonation engine propulsion concepts is reliable estimates of the performance as a function of operating conditions and fuel types. The purpose of the present work is to develop a simple analytical model for performance based on elementary gas dynamics and dimensional analysis. This model is based on experimental observations and validated against measurements reported in our companion paper, Cooper et al.[6] In developing our model we have considered only the simplest configuration of a detonation engine, a tube open at one end and closed at the other, and single-cycle operation. We realize that there are significant issues[3] associated with inlets, valves, exits and multicycle operation that are not addressed in our approach. Our goals here are to develop and validate a simple model that can provide an upper bound on the impulse expected from the simplest configuration possible.

In developing our model, we considered the following idealized representation of the processes in a single cycle of pulse detonation operation. A pulse detonation engine goes through four major steps during one cycle: the filling of the device with a combustible mixture, the initiation of the detonation, the propagation of the detonation down the tube and finally the exhaust of the products in the atmosphere through a blowdown process. A schematic of the cycle is shown in Figure 1. The pressure differential created by the detonation wave generates an unsteady thrust. The repetition of this cycle at a high frequency (ideally a few hundred Hz) creates a quasi-steady thrust.

One of the most important performance parameters of a pulsed detonation engine is the impulse delivered during one cycle. The knowledge of the impulse allows the determination of the thrust as soon as the cycle frequency is known. However, this fundamental parameter has been estimated only through numerical simulations, and the results of these computations are subject to wide variation.[5] We are motivated to develop an analytical model in order to be able to predict trends and to better understand the influence of fuel type, initial conditions, and tube size without carrying out a large number of numerical simulations. This paper presents an analytical model that was developed and validated against direct experimental impulse measurements.[6] The model provides estimates for the impulse per unit volume and specific impulse of a single-cycle pulse detonation engine for a wide range of fuels (including aviation fuels) and initial conditions.

Analytical model for impulse calculations

The impulse of a single-cycle pulse detonation engine has been determined for several mixtures using a model involving gas dynamics calculations and experimental results.

Single-cycle pulse detonation engine

During a cycle, thrust is being generated as long as the pressure inside the tube on the thrust surface (where the detonation was initiated) is greater than the atmospheric pressure. A closer look at the gas dynamics inside the tube can lead us to define four different stages in a pulse detonation engine cycle by considering the reflected wave off the interface at the open end of the tube, as depicted in Figure 1.

Boundary conditions at the open end of the tube

The analysis of the gas dynamics inside the tube requires the knowledge of what is happening when the incident detonation wave reaches the open end of the tube. The flow behind the detonation wave is subsonic and has a Mach number $M_2 = u_2/c_2$ of approximately 0.8 for typical hydrocarbon mixtures. Hence when the detonation wave reaches the open end, a disturbance

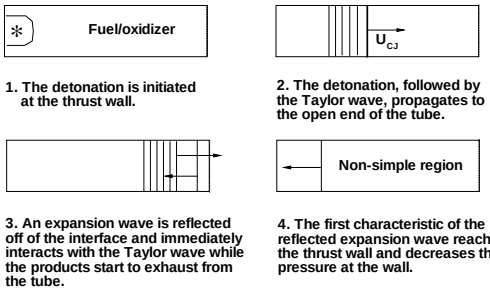

Fig. 1 Pulse detonation engine cycle.

propagates back into the tube in the form of a reflected wave. The interface at the open end of the tube can be modeled in one-dimension as a contact surface. When the detonation wave is incident on this contact surface, a transmitted wave will propagate out of the tube while a second wave is reflected back towards the thrust surface. A contact surface separates the gas processed by the incident and reflected waves from that processed by the transmitted wave. The reflected wave can be either a shock or an expansion wave. A simple way to determine the nature of the reflected wave is to use a pressure-velocity diagram as the pressure and velocity must be matched across the contact surface after the interaction. In the case of a detonation wave exiting into air at one atmosphere, the transmitted wave will always be a blast wave; the locus of solutions (the shock adiabat) is shown in Figures 2 and 3. The shock adiabat is given by the shock jump conditions for an ideal gas:

$$\frac{\Delta u}{c_1} = \frac{\Delta P/P_1}{\gamma\left(1+\frac{\gamma+1}{2\gamma}\frac{\Delta P}{P_1}\right)^{\frac{1}{2}}} \qquad (1)$$

where u is the flow velocity, c_1 is the sound speed in air, P_1 is the initial pressure, and γ is the ratio of the specific heats.

The reflected wave initially propagates back into the burnt products behind the detonation wave, gas which is assumed to be at the Chapman-Jouguet (CJ) state. The CJ states for various fuels at various equivalence ratios are also shown in Figures 2 and 3. If the CJ point is below the shock adiabat, the reflected wave must increase the pressure to match that behind the transmitted blast wave and is therefore a shock. Alternatively, if the CJ state is above the shock adiabat, a pressure decrease is required and the reflected wave is an expansion.

Hydrocarbon fuels all produce a reflected expansion wave at the open end for any stoichiometry. However, a reflected shock is obtained for hydrogen-oxygen at an equivalence ratio $\phi > 0.8$ and for very rich hydrogen-air mixtures ($\phi > 2.2$). All the reflected waves for stoichiometric fuel-oxygen and fuel-air mixtures are expansion waves with the exception of stoichiomet-

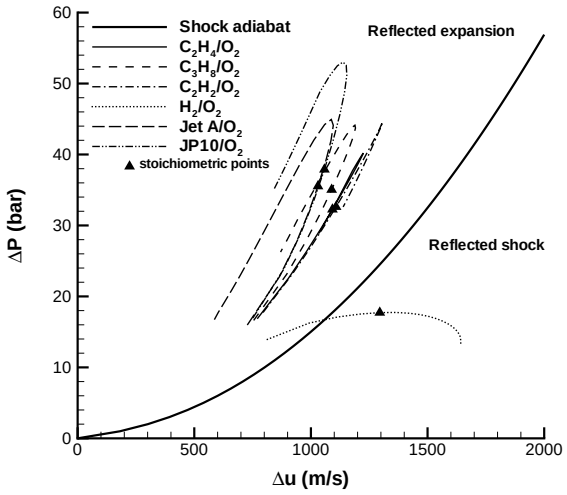

Fig. 2 Open end boundary conditions for fuel-oxygen mixtures.

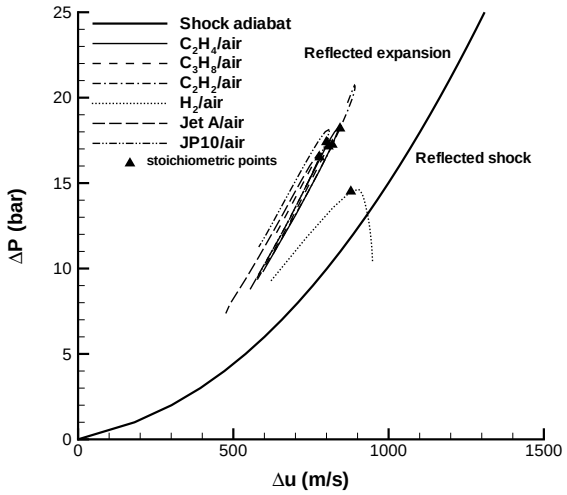

Fig. 3 Open end boundary conditions for fuel-air mixtures.

ric hydrogen-oxygen for which the reflected wave is a shock. Ultimately, following the initial interaction of the detonation wave with the contact surface, the pressure at the exit of the tube will drop as the transmitted blast wave propagates outward from the tube exit. This will produce expansion waves that will propagate back up into the tube, eventually reducing the pressure inside the tube to that of the surrounding atmosphere.

Analysis of the gas dynamics in the detonation tube

The gas dynamics inside an idealized tube (without any obstacles) can be analyzed using a distance-time (x-t) diagram shown in Figure 4. The x-t diagram displays the detonation wave propagating at the Chapman-Jouguet velocity U_{CJ} followed by the Taylor expansion wave. The first reflected characteristic from the mixture-air interface at the open end of the tube is also shown. This characteristic has an initial slope determined by the conditions at the interface, which is then modified by the interaction with the Taylor wave. Once it has passed through the Taylor wave, this first characteristic of the reflected expansion wave propagates at the sound speed of the medium c_3. The region lying behind this first characteristic is non-simple, as the reflected expansion wave interacts with the incoming Taylor wave. Two characteristic times can be defined: t_1 corresponding to the reflection of the detonation wave at the interface, and t_2 corresponding to the time necessary for the first reflected characteristic to reach the thrust surface.

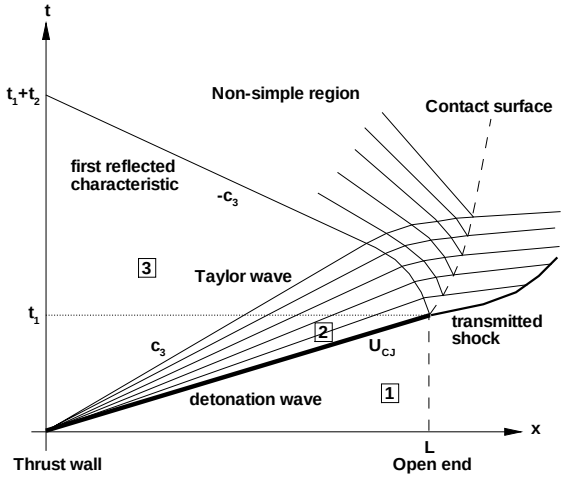

Fig. 4 x-t diagram for a detonation wave propagation and interaction with the tube open end.

The pressure differential at the thrust surface generates the single-cycle impulse. Therefore, it is interesting to focus on the pressure history at the thrust surface. When the detonation is initiated, a pressure spike is recorded (the Chapman-Jouguet pressure peak) before the pressure decreases to P_3 by the passage of the Taylor wave. The pressure at the thrust surface remains constant until the first reflected characteristic reaches the wall. The reflected expansion wave then decreases the pressure to the atmospheric value. (In some cases, the expansion wave may over-expand the flow so that the pressure is decreased below atmospheric for a period of time.)

The pressure-time trace at the thrust surface has been modeled as shown in Figure 5. The Chapman-Jouguet pressure peak is considered to occur during an infinitely short time. The pressure stays constant for a total time $t_1 + t_2$ at pressure P_3, which can be found from an isentropic flow calculation through the Taylor expansion wave. Then the pressure is affected by the

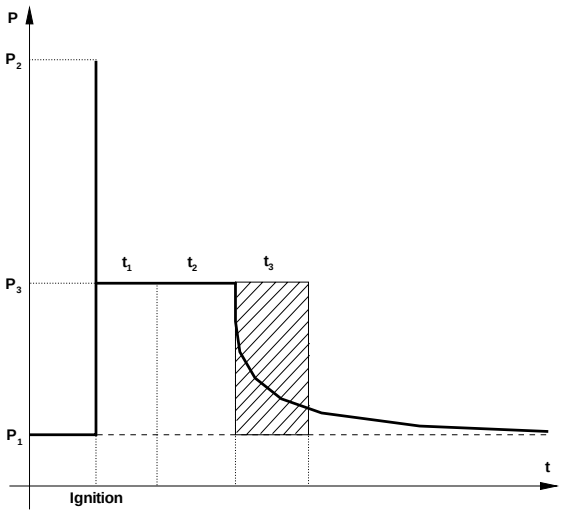

Fig. 5 Ideal modeling of the evolution of the pressure at the thrust surface with time.

reflected expansion and decreases to atmospheric. For clarity, the interaction of the transmitted wave and the contact surface with the Taylor wave is omitted on Figure 4.

Parameters for impulse calculation

The impulse of a single-cycle pulse detonation engine can be computed the following way:

$$I = A \int_0^\infty \Delta P(t)\, dt \tag{2}$$

where A is the area of the cross-section of the tube and ΔP is the pressure differential over the thrust surface. Ignition is assumed to occur at $t = 0$. Idealizing the pressure-time trace, the impulse can be decomposed into three terms:

$$I = A \left[\Delta P_3 (t_1 + t_2) + \int_{t_2}^\infty \Delta P(t) dt \right] \tag{3}$$

where t_1 is the time necessary for the detonation to reach the end of the tube of length L: $t_1 = L/U_{CJ}$, and t_2 is the time necessary for the first reflected characteristic to reach the thrust surface. The time t_2 depends primarily on the length of the tube and the characteristic velocity behind the Taylor wave, which is the sound speed c_3. Thus, it will be modeled by introducing a non-dimensional parameter α: $t_2 = \alpha L/c_3$. The last part of the pressure-time integral will be non-dimensionalized with respect to the sound speed c_3 as it is the characteristic velocity of the medium where the reflected wave propagates, and the pressure differential ΔP_3. The portion of the integral between t_2 and ∞ is modeled by introducing another time t_3, which is expressed in terms of a non-dimensional parameter β.

$$\int_{t_2}^\infty \Delta P(t) dt = \Delta P_3 t_3 = \Delta P_3 \beta \frac{L}{c_3} \tag{4}$$

The ideal model of the pressure trace is shown on Figure 5. The hatched zone represents the equivalent area of the decaying part of the pressure-time trace, $t > t_2$. Finally, the impulse can be written as:

$$I = A \Delta P_3 \left[\frac{L}{U_{CJ}} + (\alpha + \beta) \frac{L}{c_3} \right] \tag{5}$$

Determination of α

The parameter α is determined by the interaction of the reflected wave and the Taylor wave. A similarity solution can be derived to compute the time at which the first reflected characteristic arrives at the thrust surface.[7] The assumption is that the reflected wave at the interface is an expansion wave, which is the case for hydrocarbon mixtures. The flow parameters behind the detonation front (state 2), referred to as the Chapman-Jouguet (CJ) parameters, were determined through equilibrium calculations carried out using the program STANJAN.[8] The pressure P_2, the sound speed just behind the detonation wave c_2, the detonation velocity U_{CJ}, and the flow velocity behind the detonation wave u_2 were calculated. State 3 parameters were calculated using characteristics and isentropic flow conditions across the Taylor wave. The form of the equations inside the expansion fan suggests the introduction of a similarity variable $\eta = x/c_2 t$. An ordinary differential equation can then be derived for η:

$$t \frac{d\eta}{dt} + \frac{2(\gamma - 1)}{\gamma + 1} \left[\eta - \frac{u_2}{c_2} + \frac{2}{\gamma - 1} \right] = 0 \tag{6}$$

The solution to this equation with the appropriate initial conditions gives the time at which the first reflected characteristic exits the Taylor wave. It subsequently propagates at the sound speed c_3 of medium 3. The time t_2 at which it reaches the thrust surface can therefore be computed, giving the following result for α:

$$\alpha = \frac{c_3}{U_{CJ}} \left[2 \left(\frac{\gamma - 1}{\gamma + 1} \left[\frac{c_3 - u_2}{c_2} + \frac{2}{\gamma - 1} \right] \right)^{-\frac{\gamma+1}{2(\gamma-1)}} - 1 \right] \tag{7}$$

The quantities involved in this expression essentially depend on two non-dimensional parameters: γ and the detonation Mach number $M_{CJ} = U_{CJ}/c_1$. The parameters behind the shock wave (labeled 2) can be computed analytically using the ideal gas model for a CJ detonation. The resulting expression[7] for α in the ideal gas case is:

$$\begin{aligned} \alpha(\gamma, M_{CJ}) = {} & \frac{1}{2} \left(1 + \frac{1}{M_{CJ}^2} \right) \cdot \\ & \left(2 \left[\frac{\gamma - 1}{\gamma + 1} \left(\frac{\gamma + 3}{2} + \frac{2}{\gamma - 1} - \frac{(\gamma + 1)^2}{2} \cdot \right. \right. \right. \\ & \left. \left. \left. \frac{M_{CJ}^2}{1 + \gamma M_{CJ}^2} \right) \right]^{-\frac{\gamma+1}{2(\gamma-1)}} - 1 \right) \end{aligned} \tag{8}$$

Determination of β

The region lying to the right of the first reflected characteristic in Figure 4 is a non-simple region created by the interaction of the reflected expansion wave with the Taylor wave. This makes the derivation of an analytical solution for the parameter β difficult. It is, however, possible to rely on experimental data to calculate β. We considered data from our experiments[6] as well as Zitoun et al.[9] who carried out experiments aimed at measuring the impulse of pulse detonation engines using tubes of different length. The impulse was calculated for stoichiometric ethylene-oxygen mixtures by integrating the pressure differential at the thrust surface. Zitoun showed that the impulse scales with the length of the tube. The analysis of the pressure-time traces showed that the overpressure, after being roughly constant for a certain period, decreases and becomes negative before coming back to zero. The presence of this negative overpressure is attributed to an over-expansion of the flow coming out of the tube. The integration of the decaying part of the pressure-time trace had to be carried out up to a time late enough (typically greater than $20t_1$) to ensure that the overpressure is back to zero after the over-expansion. The result gives the following value for β:

$$\beta = 0.53 \tag{9}$$

Validation of the model

The model was validated against experimental data. Comparisons were made in terms of impulse per unit volume and specific impulse. The impulse per unit volume is $I_V = I/V$ where I is the single-cycle impulse and V is the volume of the tube. The mixture-based specific impulse I_{sp} is defined as the ratio of the single-cycle impulse to the product of the mixture mass $\rho_1 V$ and earth gravitational acceleration g:

$$I_{sp} = \frac{I}{\rho_1 V g} = \frac{I_V}{\rho_1 g} \tag{10}$$

The fuel-based specific impulse I_{spf} is defined with respect to the fuel mass instead of the mixture mass:

$$I_{spf} = \frac{I}{\rho_1 X_F V g} = \frac{I_V}{X_F} \tag{11}$$

where X_F is the fuel mass fraction.

Impulse per unit volume comparisons

The analytical model predictions were compared in terms of impulse per unit volume with extensive data from Cooper et al.,[6] who carried out direct experimental impulse measurements using a ballistic pendulum technique. In these experiments, detonation initiation was obtained via deflagration-to-detonation transition (DDT). Obstacles were mounted inside the detonation tube in some of the experiments in order to enhance DDT. A correlation plot showing the impulse per unit volume obtained with the model versus the experimental values is displayed in Figure 6. The values displayed here cover experiments with 4 different fuels (hydrogen, acetylene, ethylene and propane) over a wide range of initial conditions (equivalence ratio, initial pressure, and nitrogen dilution variation). The solid line represents perfect correlation between the experimental data and the model. The full symbols represent the data for unobstructed tubes, while the open symbols correspond to cases for which obstacles were used in the detonation tube. The analytical model predictions were close to the experimental values of the impulse, especially at high pressure and zero-dilution. The model assumes direct initiation of detonation, so it does not take into account any phenomenon associated with DDT. The agreement is better for cases with high initial pressure and no nitrogen dilution, since the DDT time (time it takes the initial flame to transition to a detonation) is the shortest for these mixtures. In general, the model values fall within 15% of the experimentally determined values, except for two cases, one where the model underpredicts and one where it overpredicts the impulse by about 25%. However, the model systematically underpredicts the values for the unobstructed tube experiments by 5% to 15%, except for the acetylene case, where it is about 25% too low. When obstacles are used, the experimental values are much lower and the model overpredicts them by as much as 25%, although in general the error is within 15%. The lower experimental values for cases with obstacles are caused by the additional drag created by the obstacles.

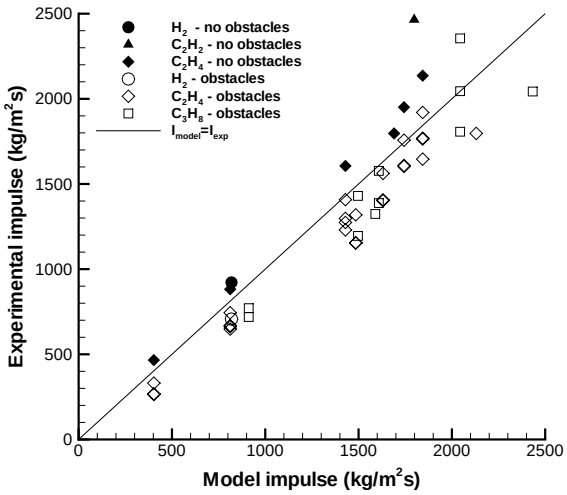

Fig. 6 Model predictions versus experimental data for the impulse per unit volume. Filled symbols represent data for unobstructed tubes, whereas open symbols show data for cases in which obstacles were used.

The value of the parameter β was checked against values obtained from the ballistic pendulum experi-

ments.[6] For stoichiometric ethylene-oxygen mixtures at 100 and 80 kPa initial pressure, the values found were 0.5 and 0.73. The first value is fairly close to the one considered in the model. The higher discrepancy with the second value is due to the DDT initiation used in the experiments. The DDT time is much shorter at 100 kPa and the process is more similar to the direct initiation assumed in the model.

The value of the parameter α was verified with the experimental pressure traces obtained at the thrust surface. The time at which the pressure starts to decrease after its constant part is compared to the time prediction using the model. The agreement is in general very good. A careful study of an experimental trace[6] revealed that the time between detonation initiation and the overpressure decrease corresponding to the blowdown process for a mixture of stoichiometric ethylene-air at 100 kPa initial pressure was 1.43 ms in a tube 1.016 m long. The corresponding calculated time (depending on α) was 1.39 ms, within 3% of the experimental estimate. Similarly, comparing with the value[9] for a tube of length 0.225 m, excellent agreement is obtained between the value of our model (313 μs) and Zitoun's data (315 μs), within 1% error.

The model parameters are relatively constant, $1.07 < \alpha < 1.13$ for all the mixtures studied here and $\beta = 0.53$. A reasonable estimate for α is a value of 1.1. The ratio U_{CJ}/c_3 for fuel-oxygen-nitrogen mixtures is approximately 2. For quick estimates of the impulse, the following approximate formula can be used:

$$I = 4.3\frac{\Delta P_3}{U_{CJ}}AL = 4.3\frac{\Delta P_3}{U_{CJ}}V \qquad (12)$$

where $V = AL$ is the volume of the detonation tube. The approximate formula reproduces the exact expressions within 2.5%.

Specific impulse and thrust comparisons

The model predictions were compared versus specific impulse and thrust measurements from Schauer et al.[10,11] Results are given in terms of fuel-based specific impulse for hydrogen-air[10] and propane-air[11] mixtures varying the equivalence ratio. Schauer et al.[10] conducted experiments in a 50.8 mm diameter by 914.4 mm long tube using a damped thrust stand. They collected data during multi-cycle steady state operation and the thrust was averaged over many cycles. Specific impulse comparison plots presented in Figure 7 for hydrogen-air and in Figure 8 for propane-air show that the impulse model predictions are fairly close to the experimental data. Two sets of data[11] are given for propane, corresponding to their most stable cases (in which the peak wave velocity was about 80% of the Chapman-Jouguet value) and most unstable, intermittent detonations. Figure 7 also includes experimental hydrogen-oxygen data from our own experiments.[7] The model gives higher values than the experiments because of the drag due to the obstacles in the DDT-initiated experiments (the model assumes direct detonation initiation). The dashed line on Figure 7 shows the boundary after which a reflected shock is obtained for hydrogen-air. The fact that the model still correctly predicts the impulse confirms the idea that the reflected shock is weak and the result in terms of pressure integration is similar to the one obtained assuming a reflected expansion wave.

The dropoff in the experimental data at low equivalence ratio is certainly due to cell size effects in the case of propane as the cell size at the lower equivalence ratios gets close to the usual limit of π times the diameter of the tube for detonation propagation; the cell size at $\phi = 0.74$ is λ=152 mm for propane-air.[12] In the case of hydrogen-air, the cell size at $\phi = 0.75$ is 21 mm, which is much smaller. A possible explanation according to the work of Dorofeev et al.[13] may be the effect of the expansion ratio of the mixture. However, calculations for lean hydrogen-air showed that the expansion ratio is always higher than the critical value defined[13] for hydrogen mixtures. Another reason may be related to the transition distance of the mixtures. Dorofeev et al.[14] studied the effect of scale on the onset of detonations and validated the $L = 7\lambda$ criterion, where L is the characteristic geometrical size and λ the cell size of the mixture. They defined the criterion $L > 7\lambda$ as a necessary condition for transition to detonation where the characteristic geometrical size L is carefully defined in the presence of obstacles. Schauer et al.[10] used a 4.8 mm diameter, 45.7 mm pitch Schelkin spiral in their pulse detonation tube to initiate detonations. Applying Dorofeev's definition results in a characteristic geometrical size of 257 mm. The cell size increases with decreasing equivalence ratio for lean mixtures and takes a value of 31 mm for hydrogen-air at an equivalence ratio $\phi = 0.67$.[12] The value of 7λ is comparable to the characteristic geometrical size of the system for this equivalence ratio, which corresponds to the first experimental specific impulse value significantly lower than the model prediction. For higher values of 7λ, i.e. lower equivalence ratios, this criterion[14] predicts no transition to detonation, which could explain the lower specific impulses obtained experimentally.[10]

Thrust can be calculated from the impulse model predictions, assuming a very simple pulse detonation engine model. The thrust T obtained is equal to the product of the single-cycle impulse per unit volume I_V with the volume of the tube V and the cycle repetition frequency f: $T = I_V V f$. Schauer et al.[10] measured the thrust delivered by a hydrogen-air pulse detonation engine operated at a frequency of 16 Hz. The corresponding thrust calculation was carried out using the analytical model and is compared with Schauer's data on Figure 9. The computation of the thrust with the model shows good agreement with the experimental data, except at low equivalence ratios because of

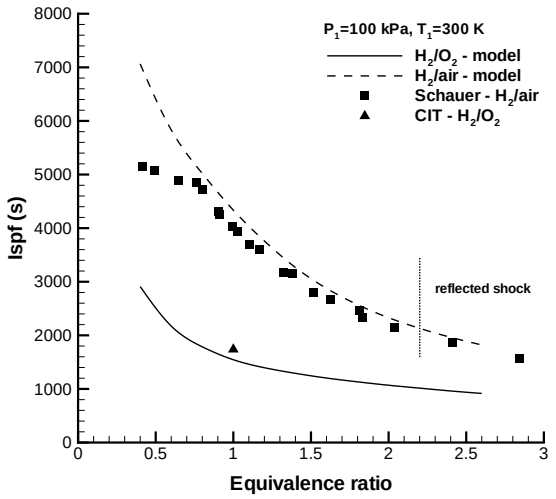

Fig. 7 Specific impulse comparison between model predictions and experimental data[7,10] for hydrogen-air varying equivalence ratio.

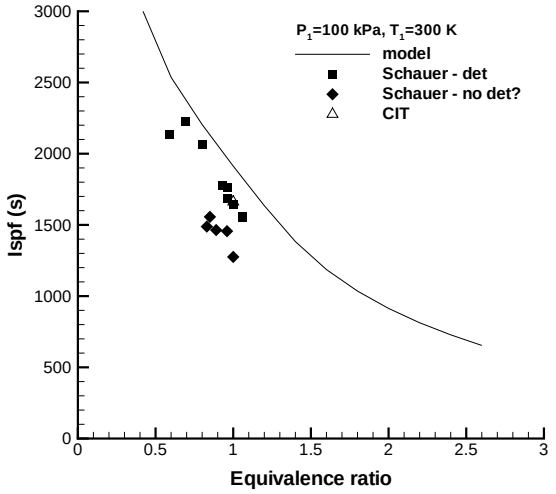

Fig. 8 Specific impulse comparison between model predictions and experimental data[7,11] for propane-air varying equivalence ratio.

the increasing transition distance discussed above.

Impulse calculations

Impulse per unit volume

Impulse calculations were carried out using the model for different mixtures including hydrocarbon fuels and hydrogen, and for a wide range of initial parameters including equivalence ratio, initial pressure and nitrogen dilution. The results were expressed in terms of impulse per unit volume of the tube, which is size-independent. The input required by the model consists of the detonation velocity U_{CJ}, the sound speed behind the detonation front c_2, the Chapman-Jouguet pressure P_2, and the ratio of the specific heats

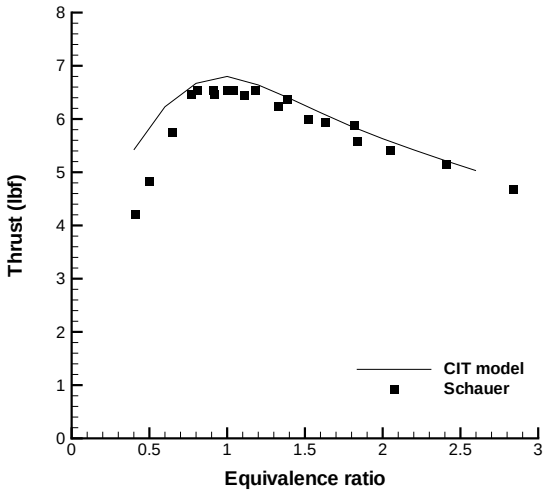

Fig. 9 Thrust calculation for a 50.8 mm diameter by 914.4 mm long hydrogen-air pulse detonation engine operated at 16 Hz. Comparison with experimental data.[10]

of the products γ. All these parameters were computed using the element-potential method for chemical equilibrium analysis implemented in the interactive program STANJAN.[8] The results are presented for the following fuels: ethylene, propane, acetylene, hydrogen, Jet A, and JP10 varying the initial pressure (Figure 10), the equivalence ratio (Figure 11) and the nitrogen dilution (Figure 12). Two sets of calculations are presented for the liquid fuels (Jet A and JP10). These fuels are in the liquid state at ambient temperature but may be heated and vaporized in the detonation tube. We have therefore examined the situations of liquid and vapor fuel separately for these cases. Two thermodynamic files were written as input to STANJAN, one defining these fuels as liquids and including a value for the density, and the other describing them as gases. These calculations define a useful range for the impulse of jet fuels and avoid having to deal with liquid fuel combustion. Regarding hydrogen mixtures, the results for hydrogen-oxygen are strictly valid for ϕ up to 0.8 and for hydrogen-air up to 2.2. For higher values of the equivalence ratio, a reflected shock is generated at the interface. However, the strength of this shock is small, which implies that the model may give a good approximation. Indeed, a ballistic pendulum experiment[7] carried out with hydrogen-oxygen resulted in the directly measured impulse being within 10% of the value predicted by the model. In these cases, the calculations are probably reasonable estimates but the reader has to keep in mind that the underlying physical assumption is not justified any more.

The initial pressure variation is characterized by a linear dependence of the impulse (see Figure 10) on

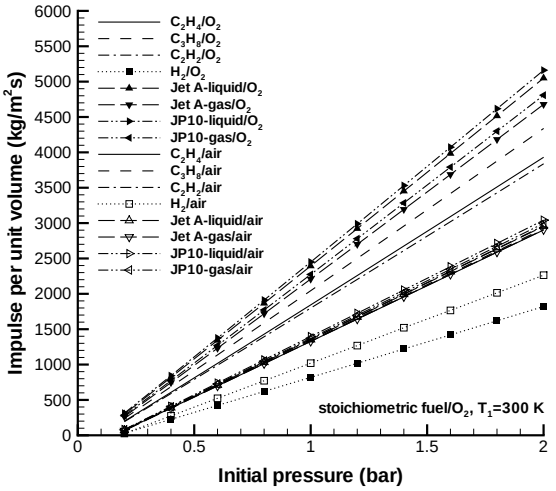

Fig. 10 Impulse per unit volume varying with initial pressure.

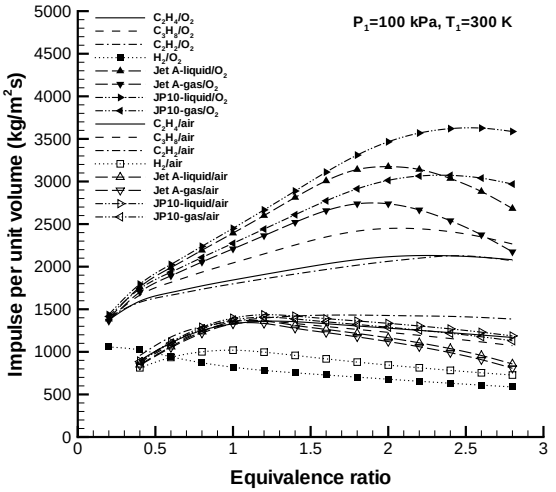

Fig. 11 Impulse per unit volume varying with equivalence ratio.

initial pressure. The impulse values for stoichiometric hydrocarbon fuel-air mixtures are very similar at all pressures. However, the computed impulse values for hydrocarbon fuel-oxygen mixtures vary over a wider range. The hydrogen cases are very different than the hydrocarbons: the impulse per unit volume is much lower due to the lower molecular mass of hydrogen, resulting in smaller density and CJ pressure. Another interesting feature is that the impulse of hydrogen-air mixtures is actually higher than the impulse of hydrogen-oxygen mixtures. The addition of nitrogen increases the molecular mass of the mixture which compensates the dilution effect, resulting in similar CJ pressures. At the same time, the dilution produces a decrease in the CJ detonation velocity and the sound speed c_3, resulting in an increase in the time of application of the pressure differential at the thrust surface and, therefore, in a higher impulse.

The plots showing the impulse per unit volume against the equivalence ratio are shown in Figure 11 and present a maximum on the rich side at a value dependent on the type of fuel, except for hydrogen. This shift of the maximum impulse on the rich side is correlated to a shift of the detonation velocity maximum and is caused by phenomena of dissociation similar to the deflagration case. In the case of hydrogen, this dissociation effect is not as prominent, so the maximum should occur closer to 1, which is the case for hydrogen-air. The hydrogen-oxygen curve decreases from the lean side to the rich side. Unlike hydrocarbon fuels, which have a molecular mass comparable to or higher than oxygen and air, hydrogen has a much lower molecular mass. Thus increasing the equivalence ratio causes a decrease in the mixture density. The CJ pressure variation is not as pronounced as for other fuels, while the detonation velocity U_{CJ} and the sound speed

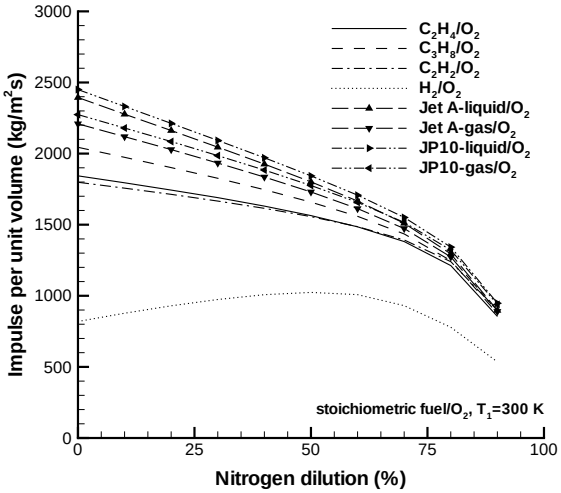

Fig. 12 Impulse per unit volume varying with nitrogen dilution.

c_3 vary significantly, increasing with ϕ. In particular, on the lean side, the density (and accordingly the pressure P_3) is high and U_{CJ} and c_3 are low, which leads to a high impulse. This dominant effect of the velocities explains the monotonically decreasing behavior of the impulse with increasing equivalence ratio in the case of hydrogen-oxygen. The nitrogen dilution for hydrogen-air mixtures reduces the variation of the characteristic velocities and enhances the influence of the pressure P_3, since the molecular mass of the mixture does not vary as much due to the presence of nitrogen.

The impulse per unit volume generated by the different fuels studied with oxygen can be ranked in all cases as follows from lowest to highest: hydrogen, acetylene, ethylene, propane, Jet A and JP10. The general trend is that the fuels with a lower hydrogen to carbon ratio

generate a higher impulse, the exception being acetylene. The case of acetylene can be explained by the lower H/C ratio and presence of a triple bond between the two carbon atoms. Reactions involving hydrocarbons with a higher carbon to hydrogen ratio will create comparatively more carbon dioxide and therefore have a higher heat of combustion. The hydrogen to carbon ratio is the following for the fuels studied here: 2 for ethylene, 2.67 for propane, 1.8 for Jet A, 1.6 for JP10, and 1 for acetylene. The combustion of hydrogen produces only water, which results in a lower heat of combustion. The results obtained for the impulse per unit volume versus the equivalence ratio are presented for an equivalence ratio range from 0.4 to 2.6. Calculations at higher equivalence ratios were carried out; however, the results obtained were unreliable because carbon production, which is very difficult to model, occurs for very rich mixtures, in particular for Jet A and JP10.

The nitrogen dilution calculations (see Figure 12) show that the impulse decreases with increasing nitrogen dilution for hydrocarbon fuels. However, as the dilution increases, the values of the impulse for the different fuels get closer to each other. The presence of the diluent masks the effect of the hydrogen to carbon ratio. The hydrogen curve is much lower due to the lower CJ pressures caused by the lower molecular mass and heat of combustion of hydrogen. Unlike for hydrocarbons, this curve has a maximum. The presence of this maximum can be explained by the two competing effects of nitrogen addition: one is to dilute the mixture, which is dominant at high dilution, while the other is to increase the molecular mass of the mixture, which is dominant at low dilution. Note that the highest value of the impulse is obtained around 50% dilution, which is close to the case of air (55.6% dilution).

Specific impulse calculations

The specific impulse was calculated for the different cases considered based on mixture mass and on fuel mass. The specific impulse was deduced from the impulse per unit volume by dividing by the product of the mixture or fuel density and earth gravitational acceleration g. The mixture-based specific impulse I_{sp} is plotted versus initial pressure, equivalence ratio, and nitrogen dilution in Figures 13, 14, and 15 respectively. Only one curve was shown for the jet fuels (Jet A and JP10) corresponding to the gaseous case. The I_{sp} curve for hydrocarbon fuels versus initial pressure decreases steeply at low pressures due to the importance of endothermic dissociation phenomena with decreasing pressure. With increasing pressure, recombination occurs and all the curves seem to tend towards a high-pressure limit. At high pressures, $\Delta P_3/P_0 \propto P_2/P_0$ and the Chapman-Jouguet pressure varies linearly with initial pressure. The parameters α and β are almost constant, and the characteristic velocities vary little with pressure (less than 5% between 0.2 and 2 bar). From Equation 5, the mixture-based specific impulse therefore tends to a limiting value.

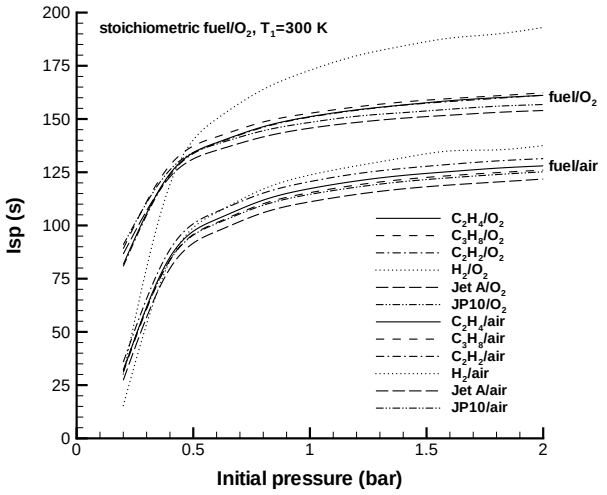

Fig. 13 Mixture-based specific impulse varying initial pressure.

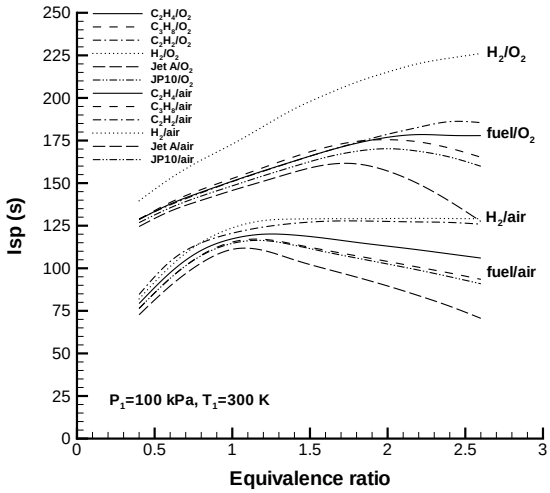

Fig. 14 Mixture-based specific impulse varying equivalence ratio.

The I_{sp} plots for hydrocarbon fuels varying the equivalence ratio are very similar to the ones obtained for the impulse per unit volume. This is expected, as the only difference is due to the density, which does not vary much for hydrocarbon fuels, which have a mass comparable to the oxidizer mass, resulting in little mixture density variation with the equivalence ratio. However, this effect is important in the case of hydrogen; the mixture density decreases significantly as the equivalence ratio increases. This accounts clearly for the shape of the monotonically increasing hydrogen-oxygen curve. The mixture density effect is masked be-

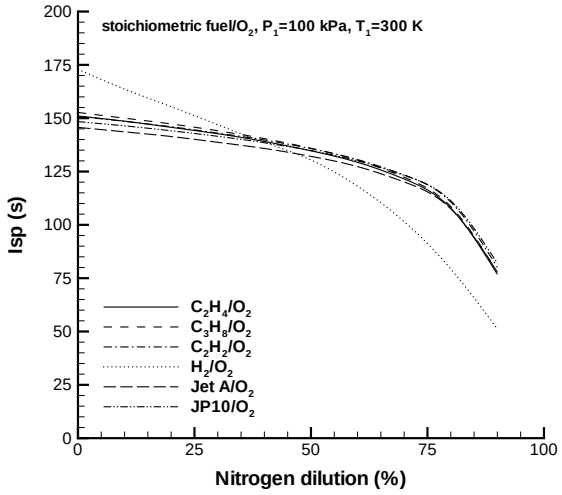

Fig. 15 Mixture-based specific impulse varying nitrogen dilution.

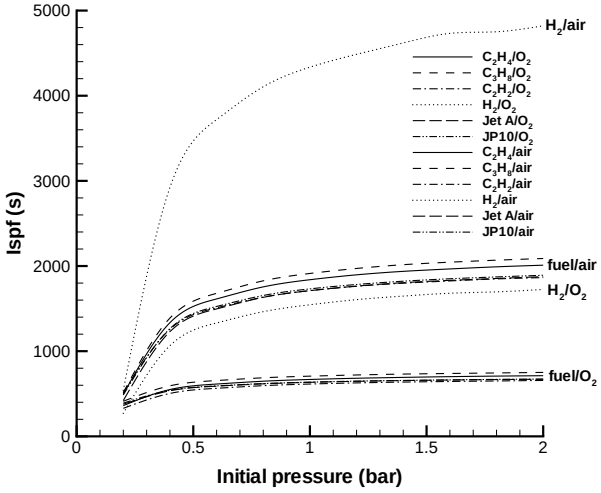

Fig. 16 Fuel-based specific impulse varying initial pressure.

cause of the nitrogen dilution in the case of hydrogen-air, which explains the nearly constant portion of the curve on the rich side.

The variation of the I_{sp} with nitrogen dilution is the same for all fuels including hydrogen. The mixture-based specific impulse decreases as the nitrogen amount in the mixture increases. The slight increase in the impulse per unit volume for hydrogen is compensated for by the molecular mass effect. Adding nitrogen to the mixture increases the molecular mass as nitrogen is a much heavier compound than hydrogen. This effect is dominant especially at low nitrogen dilution.

The fuel-based specific impulse I_{spf} is plotted versus initial pressure, equivalence ratio and nitrogen dilution in Figures 16, 17, and 18 respectively. The I_{spf} curves for initial pressure variation are very similar to the corresponding I_{sp} curves. The curves are individually shifted by a factor equal to the fuel mass fraction. Note the obvious shift of the hydrogen curves because of the very low mass fraction of hydrogen. The fuel-based specific impulse is about 3 times higher for hydrogen than for other fuels.

The equivalence ratio plots show a monotonically decreasing I_{spf} with increasing equivalence ratio. This is due to the predominant influence of the fuel mass fraction, which goes from very low on the lean side to high on the rich side, whereas the mixture-based specific impulse I_{sp} does not vary as much. The hydrogen mixtures again give much higher values compared to the hydrocarbon fuels due to the difference in mass fraction.

Similarly, the nitrogen dilution plots exhibit a monotonically increasing behavior with increasing nitrogen dilution. This behavior is once again mainly dictated by the decreasing fuel mass fraction as the nitrogen

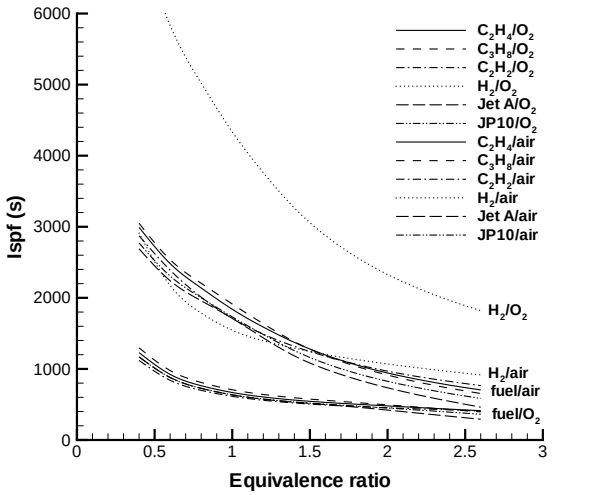

Fig. 17 Fuel-based specific impulse varying equivalence ratio.

dilution increases.

Influence of initial temperature

Temperature is another initial parameter that may significantly affect the impulse of a given pulse detonation engine. Up to now, temperature has been assumed constant at a value of 300 K in the model calculations. However, it is interesting to examine the effect of varying the temperature, especially to higher values that become of interest for flight performance or doing experiments in a heated detonation facility. Calculations were carried out using an initial mixture of stoichiometric JP10-air, which is the most interesting mixture in terms of practical applications. The impulse per unit volume (shown in Figure 19) and the mixture-based specific impulse (shown in Figure 20)

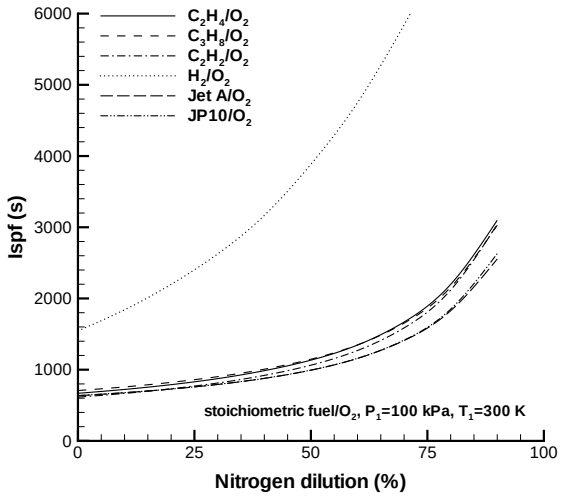

Fig. 18 Fuel-based specific impulse varying nitrogen dilution.

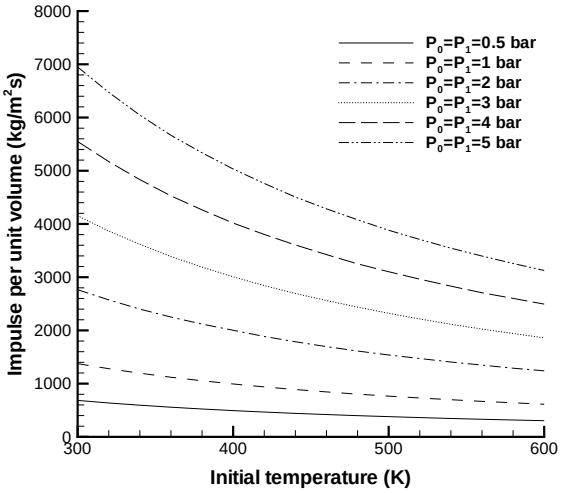

Fig. 19 Impulse per unit volume varying initial temperature for different values of the stagnation pressure.

were calculated as a function of the initial temperature for different values of the engine stagnation pressure P_1 assumed to be equal to the outside stagnation pressure P_0.

The curves showing the impulse per unit volume versus the initial temperature are decreasing hyperbolae. So increasing the temperature plays a negative role for the impulse per unit volume. This is due to the fact that the impulse per unit volume scales with the initial density. The pressure differential at the thrust surface ΔP_3 scales with P_2. The Chapman-Jouguet pressure P_2 scales as $\rho_1 U_{CJ}^2$. Given that the detonation velocity U_{CJ} and the sound speed of the products c_3 do not change significantly with initial density, the impulse per unit volume scales directly with the initial density

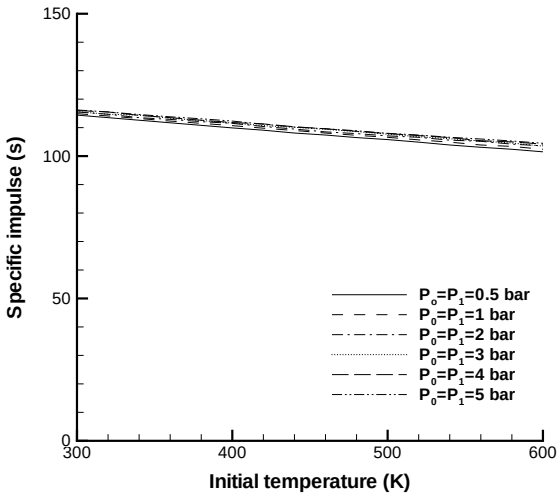

Fig. 20 Mixture-based specific impulse varying initial temperature for different values of the stagnation pressure.

ρ_1. The temperature variation is made while keeping P_1 constant, so the initial density is proportional to the inverse of the temperature. This explains why a set of hyperbolae is obtained. At the same time, the CJ pressure also scales directly with the initial pressure when the temperature is kept constant, so that the specific impulse plot should be essentially independent of initial temperature, verified in Figure 20. The specific impulse is calculated by dividing the impulse per unit volume by the initial density. Clearly specific impulse is the most useful parameter for estimating performance since it almost independent of initial pressure and temperature.

Pulse detonation engine performance

The specific impulse is a parameter that is used to compare the performance of different propulsion systems. In particular, rocket performance is usually described in terms of specific impulse. The specific impulse calculations can therefore be compared with other pulse detonation engine studies and the performance of this type of engine can be evaluated with respect to other propulsion systems.

Zitoun et al.[9] calculated the specific impulse of a multi-cycle pulse detonation engine for various reactive mixtures based on a formula developed from their experimental data for ethylene-oxygen mixtures: $I_{sp} = K\Delta P_3/(g\rho_1 U_{CJ})$. The coefficient K is estimated to be 5.4 in their study, whereas we obtained an estimate of 4.3. This accounts for the difference in the specific impulse results presented in Table 1. The analytical model impulse is about 20% lower than Zitoun's predictions.

It is also interesting to make comparisons with numerical computation estimates for the specific impulse. Numerical computations are very sensitive to the spec-

Mixture	Model I_{sp}	Zitoun et al.[9]
C_2H_4+3O_2	151.1	200
C_2H_4+3(O_2+3.76N_2)	117.3	142
C_2H_2+2.5O_2	150.9	203
C_2H_2+2.5(O_2+3.76N_2)	120.6	147
H_2+0.5O_2	172.9	226
H_2+0.5(O_2+3.76N_2)	123.7	149

Table 1 Comparison of the model predictions for the mixture-based specific impulse.

ification of the outflow boundary condition at the open end, and the numerical results are very different following the type of boundary condition adopted. Sterling et al.[1] obtained an average value of 5151 s for the fuel-based specific impulse of a stoichiometric hydrogen-air mixture in a multi-cycle simulation using a constant pressure boundary condition. Bussing et al.[3] obtained a range of values of 7500-8000 s. Other predictions by Cambier and Tegner,[4] including a correction for the effect of the initiation process, gave values between 3000 and 3800 s. More recently, Kailasanath and Patnaik[5] tried to reconcile these different studies for hydrogen-air by highlighting the effect of the outflow boundary condition. They varied the pressure relaxation rate at the exit and obtained a range of values from 4850 s (constant pressure case) to 7930 s (gradual relaxation case). Our analytical model predicts 4335 s for the specific impulse of stoichiometric hydrogen-air, and the experimental value of Schauer et al.[10] is 4024 s.

The performance of pulse detonation engines can be compared using the analytical model predictions to the performance of other types of engines. Liquid propellant rockets using LO_2-LH_2 generally have a specific impulse of 450 s.[15] More specifically, the J-2 Apollo rocket engine produced a specific impulse of 426 s,[15] while the space shuttle main engine gave a value of 363 s.[16] For comparison, the predicted performance of a hydrogen-oxygen single-cycle pulse detonation engine is 172.9 s. A significant portion of the rocket motor specific impulse is derived from conversion of thermal energy to kinetic energy in the nozzle. Without the nozzle, the thrust chamber specific impulse alone is around 240 s for hydrocarbon-oxygen rocket motors. The H-1 Saturn C-1 booster propelled by RP1-O_2 has an impulse of 257 s and the S-4 Atlas sustainer, also using RP1-O_2, has an impulse of 222 s.[16] The pulse detonation engine model specific impulse for hydrocarbon-oxygen mixtures is about 150 s. Ammonium-nitrate-based solid rockets produce specific impulses of 192 s while ammonium perchlorate solid rockets result in a higher impulse of about 260 s. As an example, the first-stage Minuteman missile motor has a specific impulse at sea level of 214 s. All these values are given here to illustrate the performance of an idealized single-cycle pulse detonation engine. The specific impulse is lower for this kind of engine than for the existing rocket engines. However, the preceding argument compares the impulse of pulse detonation engines, which are unsteady devices, with that of rocket engines, which are steady devices. The thrust delivered by a pulse detonation engine is directly proportional to the cycle repetition rate, which, therefore, plays a significant role in performance estimates.[17] No comparison is made with air-breathing propulsion systems since they involve a more detailed system analysis including inlets.

The advantages presented in terms of hardware and cycle efficiency are apparently counterbalanced by a lower specific impulse. However, care should be taken in analyzing these results. First, the specific impulse should not be the only parameter to be considered. As shown in the different impulse calculations, the result is very sensitive to the mixture molecular mass. For example, rich hydrogen-oxygen mixtures have much higher specific impulses than other mixtures, so the reader should be aware of the mass ratios when considering the fuel-based specific impulse. Based on specific impulse values, hydrogen looks like a much more efficient fuel, but a comparison of the impulse per unit volume shows that hydrogen does not produce as high an impulse as the other fuels, and, therefore, is not as efficient a propellant. This means that one parameter is not sufficient to characterize the performance of a pulse detonation engine. The specific impulses (mixture- and fuel-based) should be taken into account as well as the impulse per unit volume, which is finally the most direct size-independent characteristic parameter.

Acknowledgements

This work was supported by the Office of Naval Research Multidisciplinary University Research Initiative *Multidisciplinary Study of Pulse Detonation Engine* (grant 00014-99-1-0744, sub-contract 1686-ONR-0744), and General Electric contract GE-PO A02 81655 under DABT-63-0-0001. We thank Fred Schauer at the AFRL for sharing his data with us.

References

[1]Sterling, J., Ghorbanian, K., Humphrey, J., Sobota, T., and Pratt, D., "Numerical Investigations of Pulse Detonation Wave Engines," 31st AIAA/ASME/SAE/ASEE Joint Propulsion Conference and Exhibit, July 10–12, 1995, San Diego, CA, AIAA 95–2479.

[2]Bussing, T. R. A. and Pappas, G., "Pulse Detonation Engine Theory and Concepts," Progress in Aeronautics and Astronautics, Vol. 165, 1996.

[3]Bussing, T. R. A., Bratkovich, T. E., and Hinkey, J. B., "Practical Implementation of Pulse Detonation Engines," 33rd AIAA/ASME/SAE/ASEE Joint Propulsion Conference and Exhibit, July 6–9, 1997, Seattle, WA, AIAA 97-2748.

[4]Cambier, J. L. and Tegner, J. K., "Strategies for Pulsed Detonation Engine Performance Optimization," 33rd AIAA/ASME/SAE/ASEE Joint Propulsion Conference and Exhibit, July 6–9, 1997, Seattle, WA, AIAA 97-2743.

[5]Kailasanath, K. and Patnaik, G., "Performance Estimates of Pulsed Detonation Engines," Proceedings of the 28th International Symposium on Combustion, The Combustion Institute, July 2000, Edinburgh, Scotland.

[6]Cooper, M., Austin, J., Jackson, S., Wintenberger, E., and Shepherd, J. E., "Direct experimental impulse measurements for deflagrations and detonations," 37th AIAA/ASME/SAE/ASEE Joint Propulsion Conference, July 8–11, 2001, Salt Lake City, UT, AIAA 2001-3812.

[7]Wintenberger, E., Austin, J., Cooper, M., Jackson, S., and Shepherd, J. E., "Impulse of a pulse detonation engine: single-cycle model," GALCIT Report FM00-8, Pasadena, CA 91125, 2001.

[8]Reynolds, W., "The Element Potential Method for Chemical Equilibrium Analysis: Implementation in the Interactive Program STANJAN," Technical Report, Mechanical Engineering Department, Stanford University, 1986.

[9]Zitoun, R. and Desbordes, D., "Propulsive Performances of Pulsed Detonations," Comb. Sci. Tech., 1999, Vol. 144, pp. 93–114.

[10]Schauer, F., Stutrud, J., and Bradley, R., "Detonation Initiation Studies and Performance Results for Pulsed Detonation Engines," 39th AIAA Aerospace Sciences Meeting and Exhibit, January 8–11, 2001, Reno, NV, AIAA 2001-1129.

[11]Schauer, F., Private communication, 2001.

[12]Shepherd, J. E. and Kaneshige, M., "Detonation Database," www.galcit.caltech.edu/∼jeshep/detn_db/html/.

[13]Dorofeev, S., Kuznetzov, M. S., Alekseev, V. I., Efimenko, A. A., and Breitung, W., "Evaluation of limits for effective flame acceleration in hydrogen mixtures," Russian Research Center Kurchatov Institute-Forschungszentrum Karlsruhe Germany, Report IAE-6150/3 FZKA-6349, 1999.

[14]Dorofeev, S., Sidorov, V. P., Kuznetzov, M. S., Matsukov, I. D., and Alekseev, V. I., "Effect of scale on the onset of detonations," Shock Waves, Vol. 10, 2000, pp. 137–149.

[15]Hill, P. G. and Peterson, C. R., "Mechanics and Thermodynamics of Propulsion," Addison-Wesley, Second Edition, ISBN 0-201-14659-2, 1992.

[16]Sutton, G. P., "Rocket Propulsion Elements," Wiley-Interscience, Fifth Edition, ISBN 0-471-80027-9, 1986.

[17]Chao, T., Wintenberger, E., and Shepherd, J. E., "On the design of pulse detonation engines," GALCIT Report FM00-7, Graduate Aeronautical Laboratories, California Institute of Technology, Pasadena, CA 91125, 2001.